Published in final edited form as:
Exp Neurol. 2012 September ; 237(1): 26–35. doi:10.1016/j.expneurol.2012.06.004.

Development of AMPA receptor and GABA B receptor-sensitive spinal hyper-reflexia after spinal air embolism in rat: a systematic neurological, electrophysiological and qualitative histopathological study

Osamu Kakinohana, PhD[1], **Miriam Scadeng, MD**[2], **Jose A. Corleto**[1], **Juraj Sevc, PhD**[4], **Nadezda Lukacova, PhD**[3], and **Martin Marsala, MD**[1]

[1]Neuroregeneration Laboratory, Department of Anesthesiology, University of California, San Diego, La Jolla, CA, USA

[2]UCSD Center for Functional MRI, University of California, San Diego, La Jolla, CA, USA

[3]Institute of Neurobiology, Slovak Academy of Sciences, Kosice, Slovak Republic

[4]Institute of Biology and Ecology, Faculty of Science, P.J. Šafárik University, Košice, Slovak Republic

Abstract

Decompression sickness results from formation of bubbles in the arterial and venous system, resulting in spinal disseminated neurodegenerative changes and may clinically be presented by motor dysfunction, spinal segmental stretch hyper-reflexia (i.e., spasticity) and muscle rigidity. In our current study, we describe a rat model of spinal air embolism characterized by the development of similar spinal disseminated neurodegenerative changes and functional deficit. In addition, the anti-spastic potency of systemic AMPA receptor antagonist (NGX424) or GABA B receptor agonist (baclofen) treatment was studied. To induce spinal air embolism, animals received an intra-aortic injection of air (50–200 μl/kg). After embolism, the development of spasticity was measured using computer-controlled ankle rotation. Animals receiving 150 or 200 μl of intra-aortic air injections displayed motor dysfunction with developed spastic (50–60% of animals) or flaccid (25–35% of animals) paraplegia at 5–7 days. MRI and spinal histopathological analysis showed disseminated spinal cord infarcts in the lower thoracic to sacral spinal segments. Treatment with NGX424 or baclofen provided a potent anti-spasticity effect (i.e., stretch hyper-reflexia inhibition). This model appears to provide a valuable experimental tool to study the pathophysiology of air embolism-induced spinal injury and permits the assessment of new treatment efficacy targeted to modulate neurological symptoms resulting from spinal air embolism.

Correspondence: Martin Marsala, M.D. Neuroregeneration Laboratory, Department of Anesthesiology, University of California - San Diego, Sanford Consortium for Regenerative Medicine, 2880 Torrey Pines Scenic Drive, La Jolla, CA 92037, mmarsala@ucsd.edu, Ph (office): 858-822-3805, Ph (lab): 858-534-7380, Fax: 858-822-3249.

Keywords

spinal cord; air embolism; paralysis; spinal infarcts; spasticity; Hoffmann reflex; AMPA receptor antagonist; GABA B receptor agonist

INTRODUCTION

Decompression illness (DCI), commonly known as diver's disease, is a systemic disease resulting from formation of bubbles in the tissues or circulation because of inadequate elimination of inert gas, mostly nitrogen, after diving. Clinically, patients typically present with two common types of symptoms. *Type I*: joint pain only (shoulder, elbow, hip and/or knee), skin (cutis marmorata), lymphatic (pitting edema) or *Type II:* cardiopulmonary (chokes) or neurologic (paralysis) (Barratt, et al., 2002, Barratt and Van Meter, 2004). The most commonly affected areas of the central nervous system are the lower thoracic spinal cord (Barratt, et al., 2002, Tournebise, et al., 1995) and/or the brain territory supplied by the middle cerebral artery or vertebral-basilar arterial system (Barratt, et al., 2002). Qualitative neurological evaluation in patients with Type II-spinal injury show the occurrence of spasticity in more than 50% of patients (Calder, et al., 1989, Kim, et al., 1988, Tournebise, et al., 1995).

It is believed that the mechanism of ischemic spinal cord injury in patients with DCI can be the result of **i)** arterial gas embolism after pulmonary barotraumas or right to left shunts (Francis, et al., 1990, Francis, et al., 1989), **ii)** gas emboli presence or formation in the spinal vertebral venous system (Hallenbeck, 1976), or **iii)** increased leukocyte adhesiveness and vascular permeability resulting from local release of chemotactic and vasoactive substances (Ward, et al., 1990). Independent of the nature of how the decrease in local spinal circulation is induced, i.e., spinal venous respiratory arterial air embolism or changes in local vascular permeability, the resulting neurological dysfunction and corresponding spinal neurodegenerative changes show quite a predictable pattern.

Clinical studies show that functionally a predominant deficit after DCI-induced spinal injury is characterized by the presence of paretic changes frequently combined with muscle spasticity. In a significant population of patients, this undiagnosed muscle spasticity remains unchanged even after rapid recompression-hyperbaric oxygen therapy (Calder, et al., 1989, Tournebise, et al., 1995). Histopathological analyses of spinal cord tissue in patients with DCI show the presence of disseminated necrotic cavities affecting both white and gray matter areas and distributed through the cervical, thoracic and/or lumbar spinal cord (Calder, et al., 1989, Tournebise, et al., 1995).

Using animal models of DCI, comparable development of spinal infarcts affecting both white and gray matter and corresponding neurological deficit was described. The most widely used model of DCI is the swine model. In this model, using a compression chamber, a simulated dive into 200 feet of seawater (612.6 kPa) with a decompression rate of 60 $fsw.min^{-1}$ is typically used to induce DCI. Animals show signs of motor dysfunction and dysaesthesia during the first 2–7 min after decompression (Broome and Dick, 1996). Histopathological analyses in pigs with DCI show the presence of spinal parenchymal hemorrhages and spongiosis at 24 hrs after induction of DCI (Broome and Dick, 1996) and with fully developed necrotic foci several days after injury (Barratt, et al., 2002).

Using a rat model of DCI similar spinal neuropathological changes were seen. Thus, in animals exposed to a simulated dive to 165 feet and decompression rate at 3.7–9.9 feet/sec, the presence of "space occupying lesions" was seen primarily in white matter immediately after decompression followed by the appearance of focal necrosis and demyelination

(Hyldegaard, et al., 1994). In the same model, electrophysiological analysis of spinal monosynaptic reflex and motor evoked potentials showed a decrease in monosynaptic reflex responses during the first 60 min after dive (Marzella and Yin, 1994).

Interestingly, despite the well-documented appearance of spasticity in patients with DCI, there is no systematic experimental data available which would characterize the time course, qualitative/quantitative characteristics as well as the pharmacology of DCI-induced spasticity. In our previous studies, we have developed and characterized a computer-controlled muscle resistance meter which permits the objective assessment of changes in stretch reflex activity in fully awake adult Sprague-Dawley rats (Marsala, et al., 2005). Using this system, we have demonstrated the development of muscle spasticity (in addition to muscle rigidity) in a rat aortic balloon occlusion model of spinal ischemic injury (Taira and Marsala, 1996). Spinal histopathological changes in rats after aortic occlusion are characterized by a selective loss of spinal GABA-ergic inhibitory interneurons in the lumbosacral segment, however, with a continuing presence of functional α-motoneurons (Kakinohana, et al., 2006, Marsala, et al., 2004).

The above documented mechanism of spinal ischemic spasticity, i.e., local segmental loss of inhibition and resulting exacerbated α-motoneuron activity, appears to bare at least some of the pathological/functional hallmarks of muscle spasticity seen in patients with DCI. First, as discussed, spinal cord histopathological changes in DCI patients and experimental models can be presented as local areas of neuronal loss; thus, loss of local inhibitory interneurons can contribute to the development of spasticity. Second, clinical treatment studies show that patients with muscle spasticity of different etiology, including spinal trauma, ischemia multiple sclerosis or amyotrophic lateral sclerosis, show clinically effective suppression of spasticity after spinal baclofen treatment suggestive of a general role of local loss of GABA-ergic inhibition (Beard, et al., 2003, Kita and Goodkin, 2000, Krach, 2001).

Accordingly, in our present study, we aimed to: i) develop a spinal air embolism model in adult Sprague-Dawley rats, ii) characterize functionally and electrophysiologically the presence of muscle spasticity in rats at different time points after air embolism-induced spinal injury, iii) characterize corresponding spinal histopathological changes and post-mortem spinal cord MRI, and iv) measure the degree of anti-spasticity effect after systemic treatment with AMPA receptor (GluA1–GluA4) antagonist NGX424 and GABA B receptor agonist baclofen.

MATERIAL AND METHODS

Animals

These studies were carried out under protocols approved by the Institutional Animal Care and Use Committee of the University of California, San Diego (La Jolla, CA, USA) and were in compliance with the Association for Assessment of Laboratory Animal Care guidelines for animal use. All studies were performed in such a manner as to minimize group size and animal suffering.

Induction of spinal air embolism

Male Sprague-Dawley rats (B.W.: 350–370 g) were anesthetized with 2% isoflurane. A 2F Fogarty balloon catheter was placed from the left femoral artery to the descending thoracic aorta with the tip of the catheter placed just above the truncus coeliacus (7.5 cm from the femoral artery insertion point). Inflation of the balloon catheter was used to prevent kidney and intestinal embolization after injection of air into the descending thoracic aorta (see Fig. 1). A PE10 catheter (I.D. 0.28 mm) was then placed from the left carotid artery to the descending thoracic aorta with the tip of the catheter reaching the Th 7–8 level (5.0–5.5 cm).

After systemic heparinization (200 IU) through the PE10 catheter the end of the catheter was connected to the 250 μl syringe interconnected to the microsyringe injector. After cannulations, the position of the rat was changed from the supine to prone position. The balloon catheter was then inflated with 50 μl saline and air (50, 100, 150 or 200 μl/kg) was injected into the aorta through the PE10 catheter at a rate of 50 μl/min. After air embolism, catheters were removed and animals are allowed to recover and survive for 3 weeks. Manual bladder expression (crede's maneuver) was carried out in 12 hr intervals for 1–2 weeks in animals with developed paraplegia.

Evaluation of neurological function

The recovery of motor function was evaluated daily using a 21-point open field locomotor scale (21=complete recovery; 0=complete loss of motor and sensory function) (Basso, et al., 1996). BBB scores categorize combinations of rat hindlimb movements, trunk position and stability, stepping, coordination, paw placement, toe clearance, and tail position, representing sequential recovery stages that rats attain after spinal injury/air embolism.

Motor evoked potentials and Hoffmann reflex recordings

Motor evoked potentials (MEPs)—To record MEPs, animals were anesthetized (90 mg/kg) and maintained with ketamine (100 mg/kg/h, i.m.). Selection of ketamine anesthesia was based on previous studies reported from other laboratories which demonstrate a minimal suppressive effect on MEPs and Hoffmann reflex (Ho and Waite, 2002, Thompson, et al., 1998). Depth of anesthesia was verified periodically by the absence of corneal reflexes, whisker tremor and the pinna reflex. MEPs were elicited by transcranial electrical stimulation (20 V, 200 μs; ISOSTIMTM A320, WPI, Sarasota, FL, USA) of the motor cortex using percutaneous stainless steel stimulating electrodes. Responses were recorded from the gastrocnemius muscle using silver needle (22G) electrodes (distance between recording electrodes was 1 cm) connected to a preamplifier (HS4 fiber optic Bioamp Headstage, WPI) and amplified using DB4 fiber optic amplifier (WPI). Sampling rate was 80 kHz and filter bandwidth was set at 100–10,000 Hz. MEPs were recorded in 7-day intervals and stored on a PC for analysis. MEPs were recorded and analyzed in all experimental groups.

Hoffmann reflex (H-reflex)—Animals were anesthetized and maintained with ketamine (100 mg/kg, i.m.) as described for MEPs recording. For stimulation of the H-reflex, a pair of needle electrodes was transcutaneously inserted into the vicinity of the tibial nerve. For recording, a pair of silver needle electrodes was placed into the right foot muscles. The tibial nerve was stimulated with increasing stimulus intensity (0.1–10 mA in 0.5 mA increments, 0.1 Hz, 0.2 ms; WPI; Isostim A320). The threshold for both the M and H waves was determined and Hmax/Mmax ratio calculated. Recording of H-reflex and MEPs were performed during the same session.

Assessment of rate-dependent depression of H-reflex: Recording of RDD was performed as previously described (Boulenguez, et al., 2010). Briefly, the tibial nerve was stimulated for 0.2 ms at 0.1 Hz with increasing current intensities until a stable Mmax and a maximal H response was determined. A train of 20 stimuli at 0.1, 0.5, 1, 2 and 5 Hz was then used in order to measure the RDD, with 2 min intervals between each train of stimulations so that a whole series of measurements lasted about 15–20 min. In order to determine the level of RDD at different frequencies, we discarded responses to the first three stimulations necessary for the depression to occur and expressed all the responses as percentages relative to the mean response at 0.1 Hz in the same series of measurements.

Hoffmann reflex and RDD were only measured in animals with clinically defined spasticity (see next paragraph).

Measurements of muscle spasticity

Starting at 2–3 days after air embolism, animals were tested for the appearance of spasticity. The presence of spasticity was identified as an increase in ankle resistance during 3 sec lasting computer-controlled ankle dorsiflexion (i.e., active ankle resistance), which correlated with increased EMG activity measured in the gastrocnemius muscle during the same time frame.

Direct measurement of ankle resistance during computer-controlled ankle dorsiflexion was performed as described previously (Marsala, et al., 2005). Briefly, rats after spinal air embolism were individually placed in a plastic restrainer, and one hindpaw was securely fastened to the paw attachment metal plate, which is interconnected loosely to the "bridging" force transducer (LCL454G, 0–454 g range; or LCL816G, 0–816 g range; Omega, Stamford, CT). After a 20 min acclimation period, rotational force was applied to the paw attachment unit using a computer-controlled stepping motor (MDrive 34 with onboard electronics; microstep resolution to 256 microsteps/full step; Intelligent Motion Systems, Marlborough, CT), causing the ankle to dorsiflex (Fig. 3A). The resistance of the ankle was measured during 40° of dorsiflexion during 3 sec (13.3° s^{-1}), and data were collected directly to a computer using custom software (Spasticity version 2.01; Ellipse, Kosice, Slovak Republic).

To identify the mechanical component of measured ankle resistance, all animals were anesthetized with 2.5–3% isoflurane at the end of the experiment and the relative contribution of mechanical vs. neurogenic component (isoflurane-sensitive) was calculated. Data generated before and after NGX424 or baclofen treatment were expressed as % of neurogenic component contributing to measured resistance (see Fig. 3 for details). Each recorded value was the average of three repetitions. To record EMG activity, a pair of tungsten electrodes were inserted percutaneously into the gastrocnemius muscle 1 cm apart. EMG signals were bandpass filtered (100 Hz to 10 kHz) and recorded before, during, and after ankle dorsiflexion. EMG responses were recorded with an alternating current-coupled differential amplifier (model DB4; World Precision Instruments, Sarasota, FL) and stored on a computer for subsequent analysis. EMG was recorded concurrently with ankle resistance measurement during dorsiflexion, and expressed as the average of three measurements. Digitized EMG signal was full-wave rectified, and values within given time interval (bin) were averaged and used for statistical analysis. Similarly as for ankle resistance, integrated EMG data recorded before and after induction of isoflurane anesthesia were used to determine the maximum possible effect.

Post mortem magnetic resonance imaging

Dissected rat spinal cords were imaged immersed in perfluorocarbon (Solvay Solexis Bollate (MI), Italy). Images were acquired in a horizontal bore 7-T MRI (GE Medical Systems Milwaukee), with a 10 mm transmit/receive MR imaging surface coil using a 2D FSPGR sequence TR/TE=10/2.9, FA 20°, FOV 10 mm, matrix 160×128 and a slice thickness of 100 microns. Imaging time was 60 min.

Three-dimensional rendering and anatomical measurements—The image data sets were manually volume and surface rendered using AMIRA software (Mercury Computer Systems, Chelmsford, Massachusetts) to produce quantitative three-dimensional models. From these computed models dimensions such as infarct area/volume can be determined.

Perfusion fixation and tissue processing

At the end of the survival periods, rats were anesthetized with pentobarbital (40 mg/kg; i.p.) and transcardially perfused with heparinized saline (100 ml) followed by 4% paraformaldehyde in 0.1 M phosphate buffer (PB; 500 ml). The spinal cords were dissected and postfixed in the same fixative overnight at 4°C. After postfixation, tissue was cryoprotected in graded sucrose solutions (10, 20 and 30%). Frozen transverse spinal cord sections (10–30 μm) were then cut. For immunohistochemistry, free-floating sections (30 μm) were placed in PBS (0.1 M; pH=7.4) containing 5% normal goat or donkey serum (NGS, DS), 0.2% Triton X-100 (TX), for 2 hr at room temperature to block non-specific protein activity. This was followed by overnight incubation at 4°C with primary antibodies: mouse NeuN (NeuN; 1:1000; Chemicon Inc., Temecula, CA, USA); mouse anti-ED1 to identify activated macrophages/microglia (ED1; 1:1000; Chemicon Inc., Temecula, CA, USA); rabbit anti-GFAP (GFAP; Chemicon Inc., Temecula, CA, USA). After incubation with primary antibodies, sections were washed 3x in PBS and incubated with fluorescent-conjugated secondary goat anti-rabbit or goat anti-mouse antibodies (Alexa 488, 594, 680; 4 μl/ml; Molecular Probes, Eugene, OR, USA). All blocking and antibody preparations were made in 0.1 M PBS/0.2% TX/5% NGS. For multiple labeling experiments, primary antibodies from different species were applied simultaneously, followed by application of secondary antibodies conjugated to different fluorescent markers. For general nuclear staining DAPI (3 μl/ml) was added to the final secondary antibody solutions. After staining, sections were mounted on slides, dried at room temperature and covered with Prolong anti-fade kit (Molecular Probes). Alternative sections were mounted on Silane Prep slides and stained with Klüver-Barrera staining method to assess general neuronal and neuropil morphology.

Brightfield images of Klüver-Barrera stained sections were captured using a Leica DMLB Microscope (40x objective, Olympus firewire camera). Analysis of fluorescence sections was performed using standard fluorescence and confocal microscopy (Fluoview 1000, OLYMPUS).

Statistical analysis

Neurological outcome was analyzed using mixed-design ANOVA (group x time post-air embolism), followed by comparisons of the simple main effects among individual groups. A p value of 0.05, Bonferroni-corrected for multiple comparisons, was considered significant. Neurophysiological data (MEPs and Hoffmann reflex, RDD) were analyzed using unpaired student's t-test.

RESULTS

Progressive development of paraplegia in rats after spinal air embolism (Fig. 2A)

Animals that received 50 or 100 μl of intra-aortic air injection showed transient motor dysfunction during 7–10 days after embolism and it was then followed by complete functional recovery (BBB score 21). In contrast, animals receiving 150 or 200 μl of intra-aortic air injection displayed consistent motor dysfunction or presence of fully developed paraplegia (BBB score 4.8–10). In 4 of 8 animals in the 150 μl group and 5 of 8 animals in the 200 μl group, a progressive increase in baseline motor tone (rigidity) and spasticity (increased muscle resistance during ankle dorsiflexion--see following paragraph) in the lower extremities was seen at 7–21 days after air embolism.

Interestingly, independent of the volume of air injected, animals in all experimental groups showed near normal neurological function during the first 30–60 min after recovery from

anesthesia. Progressive loss of neurological function was then seen and typically was fully developed between 1–4 hrs after induction of air embolism.

Changes in motor evoked potentials and Hoffmann reflex after SAE (Fig. 2B–E)

Recording of motor evoked potentials from the gastrocnemius muscle after electrical stimulation of the motor cortex was performed at 2–3 weeks after SAE and showed 2 types of recording patterns. First, in 3 of 8 animals in the 200 μl group and in 2 of 8 animals in the 150 μl group, no responses were recorded at stimulation intensities of 0.8–8 mA (Fig. 2B; lower trace-no response). Other animals in both experimental groups showed on average a 30–120% increase in recorded MEP amplitudes when compared to naïve controls (control −3.56±0.35 mV, air embolism −10.79±0.50 mV; $p<0.01$; n=11), (Fig. 2B, middle trace-increased response). In the 50 μl group and the 100 μl group, no significant differences were detected.

Hoffmann reflex was recorded in animals with identified spasticity (4 animals in the 200 μl group and 5 animals in the 150 μl group; see following paragraph). In those animals, a significant increase in H/M ratio was measured (Fig. 2C, Table 1). When compared with control animals, a significant loss of rate-dependent-depression (RDD) was recorded at stimulation frequencies of 0.5, 1 and 5 Hz (Fig. 2D,E; Table 2).

Development of muscle spasticity in rats after SAE (Fig. 3A–C)

To identify the presence of muscle spasticity, ankle rotational (40°) force was applied on the left paw and the ankle rotated 40° at a velocity of 3 cm/sec in fully awake animals. The resistance of the ankle during rotation and correlative changes in EMG activity in the gastrocnemius muscle were measured (Fig. 3A). Compared to control animals, a clear appearance of evoked EMG activity was measured in 4 animals from the 200 μl air embolism group and in 5 animals from the 150 μl group (compare EMG tracing in Fig. 3B to C). Similarly, compared to control animals, increased muscle resistance was also measured during ankle dorsiflexion and ranged between 20–150 g (compare Muscle Resistance tracing in Fig. 3B to C).

Amelioration of SAE-induced spasticity by systemic treatment with GABA B receptor agonist baclofen and AMPA receptor antagonist NGX424 (Fig. 3C–H; Fig. 4)

In animals with identified spasticity, the anti-spastic effect after systemic treatment with AMPA receptor antagonist NXG424 (12 mg/kg/i.p.) was tested. Ten to fifteen min after injection, a clear suppression of spasticity response was measured (compare tracing in Fig. 3C to D; Fig. 4). Similarly, systemic treatment with GABA B receptor agonist baclofen (20 mg/kg/i.p.) led to a potent anti-spasticity effect as evidenced by suppression of EMG response and muscle resistance measured during ankle dorsiflexion (compare tracing in Fig. 3F to G). To identify the contribution of the mechanical component in measured resistance, animals were anesthetized with isoflurane (2%) at the end of experiment. After isoflurane induction a near complete loss of EMG activity was seen while mechanical resistance resulting from ankle joint ankylosis remained unaffected (compare tracings in Fig. 3D to E and G to H).

Development of disseminated spinal necrotic foci after SAE (Fig. 5A–I)

Using postmortem MRI of dissected whole spinal cord, a rostro-caudal and dorso-ventral distribution of necrotic foci was identified in animals injected with 150–200 μl of air (Fig. 5A; red areas). The size of low density areas corresponding to disseminated necrotic lesions ranged between 200 μm to several millimeters in size and were localized in the lower thoracic to sacral spinal cord segments.

Histological staining with the Klüver-Barrera method of transverse spinal cord sections taken from L2–L6 spinal segments in animals after 150 and 200 μl of aortic air injections showed the presence of irregularly distributed areas of increased cellularity at 3 weeks after air embolism. We speculate that this increased cellularity at the site of injury is likely the result of local proliferation of microglia and/or astrocytes. If the areas of increased cellularity were localized in the gray matter, a clear loss of neurons was identified in the same regions (compare Fig. 5B to C; red dashed circle). Immunofluorescence staining of the adjacent sections with NeuN antibody confirmed the presence of focal neuronal loss and was typically localized in the intermediate zone (lamina VII) or in the ventral horns (lamina VIII and IX) (compare Fig. 5D to E; yellow dashed circle). Staining with ED1 antibody, which recognizes the presence of activated microglia and macrophages, showed an intense accumulation of ED+ elements in infarcted regions (compare Fig. 5F to G). In addition to gray matter areas with ED immunoreactivity (Fig. 5G; blue arrows), a clear presence of ED+ cells was identified bilaterally or unilaterally in dorsal funiculus (i.e., the region of dorsal corticospinal tract in rat) and in lateral white matter (Fig. 5G; yellow arrows). Double immunostaining with ED1 and GFAP antibody showed the presence of activated hypertrophic astrocytes (Fig. 5I; yellow arrows) in perinecrotic regions infiltrated with ED+ cells.

In animals injected with 50 or 100 μl of intra-aortic air, a similar qualitative histopathological picture was seen, however, the regions of neuronal loss and corresponding inflammatory changes were more discrete (data not shown).

DISCUSSION

Spinal arterial air embolism model characterization

In our current study, intra-aortic air injection was used to induce air embolism in the thoraco-lumbar spinal arterial system. To prevent air embolism in other organ systems (gut, liver, kidney) and the lower extremities, an aortic balloon occlusion catheter was placed above the truncus coeliacus and inflated just before injection of the air into descending thoracic aorta. As demonstrated, animals injected with the intra-aortic air volumes of 200 μl showed the most severe neurological dysfunction qualitatively, presenting as flaccid (with no motor tone) or spastic paraplegia which remained unchanged for a minimum of 21 days. Interestingly, the majority of animals showed near normal motor function during the first 30–60 min after air injection and only then displayed progressive loss of motor dysfunction. We speculate that shortly after air injections large size air emboli are formed occluding primarily the radicular arteries which feed the thoraco-lumbar regions of the spinal cord. Because of a well-developed longitudinal spinal arterial system in rats (Schievink, et al., 1988) composed of one anterior and 1–2 posterior spinal arteries, the selective occlusion of only a limited number of radicular arteries has no ischemia-inducing effect due to continuing patency of the longitudinal spinal arteries. In the subsequent phase, large air emboli are likely fractionated and smaller emboli reach the spinal penetrating arterioles. Because penetrating arterioles have no collaterals (Rubinstein and Arbit, 1990, Woolen and MIllen, 1955), this leads to development of a local, disseminated type of spinal necrotic foci affecting both the white and gray matter.

In previous studies, a similar approach was used to induce unilateral brain air embolism in swine by injecting 5 ml of air into the internal carotid artery (Medby, et al., 2002). In that study analysis of microdialysis samples collected from the cisterna magna showed a significant elevation in lactate-pyruvate ratio, indicative of anaerobic metabolism. Thus, intra-arterial air injection can effectively be used to induce local vascular occlusion. Because of well-documented limited tolerance of CNS tissue to ischemic/anoxic episodes, it leads to a predictable irreversible cellular degeneration in affected spinal cord regions.

Histopathological changes in animals with SAE

Consistent with human clinical data and experimental data from swine or rat DSI models, the neurodegenerative changes in the spinal cord at various time points after induction of spinal air embolism showed similar qualitative profile. Thus, using in situ postmortem MRI, the presence of irregular disseminated low-density necrotic foci localized in both the white and gray matter was identified. The size of the foci varied and ranged from 50–200 μm to several millimeters. There was no apparent regularity in the distribution of these lesions with some animals showing the majority of foci in the white matter while others in the gray matter or combination of both. The majority of identified necrotic foci were distributed between mid-thoracic to sacral spinal segments. Qualitative analysis showed a localized loss of neurons or white matter axons and an intense activation of microglia/macrophages seen in the same regions if analyzed at 3 weeks after air embolism. This secondary post-degenerative picture is consistent with the cellular neuroinflammatory changes seen in focal brain or spinal ischemia models induced by transient or permanent arterial occlusion (Gregersen, et al., 2000, Mabuchi, et al., 2000, Matsumoto, et al., 2003).

Variable changes in motor evoked potentials and H-reflex in animals with SAE-induced paraplegia

Recording of motor evoked potentials from gastrocnemius muscle after electrical stimulation of motor cortex showed 2 quantitatively different patterns. In the first group, no MEP response was recorded even after a relatively high intensity stimuli (8 mA). In the second group, paradoxically, increased amplitudes of MEPs were recorded. While not systematically analyzed with respect to the distribution of spinal neurodegenerative changes, we speculate that the loss of MEPs was likely caused by i) documented infarcts in the descending motor tract regions (corticospinal and/or rubrospinal) and/or ii) loss of α-motoneurons between L4–L6 spinal segments (i.e., the primary neuronal pools innervating sciatic nerve). The increase in MEPs likely reflects a continuing connectivity of descending motor tracts (pyramidal but also extrapyramidal) to corresponding persisting segmental interneurons/α-motoneurons, however, with a loss of local segmental inhibitory interneurons. We have reported a comparable increase in MEPs in rats with aortic occlusion-induced spasticity (Marsala, et al., 2004).

Changes in H-reflex were analyzed only in animals with identified muscle spasticity. These animals showed an increase in H/M wave ratio, loss of rate-dependent depression (RDD) of the H-reflex and remained unchanged for minimum of 3 weeks after appearance of spasticity. Similarly as for MEPs, the magnitude in H-reflex increase and loss of RDD at higher frequencies of peripheral nerve stimulation (0.5–5 Hz) was similar as seen in rat models of spinal ischemia-induced muscle rigidity and spasticity (Kakinohana, et al., 2006, Matsushita and Smith, 1970). Comparable development of increased α-motoneuron activity in a dog spinal ischemic injury model of muscle rigidity was reported (Gelfan, 1966).

Accordingly, we speculate that the increase in H-reflex in animals with a spastic form of SAE-induced paraplegia is in part the result of local loss of segmental inhibition; in addition, the loss of descending tract mediated activation of local segmental inhibitory circuits can be involved.

Development of spasticity in animals with SAE

In our previous studies, we have developed and characterized a computer-controlled ankle-rotation device which permits the objective measurement of peripheral muscle resistance before and during ankle rotation in fully awake rats (Marsala, et al., 2005). Using this system, we have demonstrated the development of progressive spasticity and rigidity in rats after exposure to an injurious interval (10 min) of spinal ischemia (Kakinohana, et al., 2006,

Marsala, et al., 2005). Using a comparable ankle torque measurement system, development of spasticity after contusion injury of the midthoracic spinal cord in a rat was reported (Bose, et al., 2002).

In our current study, rats with SAE-induced paraplegia which displayed clinical signs of spasticity were selected and used for spasticity measurement using an ankle-rotation muscle resistance meter. Similarly as we have seen in animals with spinal ischemic spasticity, a clear increase in ankle resistance which correlated with exacerbated EMG activity during muscle stretch (i.e., during ankle rotation) was measured in SAE-injured spastic rats. The first signs of spasticity were typically seen 2–3 days after spinal air embolism and were fully developed 5–10 days after the onset of spasticity. After this period, spasticity remained unchanged for a minimum of 3 weeks after induction of SAE (i.e., the longest time point after SAE tested in our current study).

This qualitative picture of chronic spasticity appears to parallel the spasticity described in patients with DSI. Several clinical studies have demonstrated that even after rapid recompression (2–3 hrs after dive) and significant functional-motor recovery the presence of chronic spasticity remains one of the major qualitative deficits (Calder, et al., 1989, Kim, et al., 1988, Tournebise, et al., 1995).

Pharmacology of SAE-induced spasticity

In our previous studies, we have demonstrated that the spasticity resulting from selective spinal ischemia-induced ablation of segmental inhibitory interneurons (primarily GABE-ergic) is effectively ameliorated by: i) spinal delivery of GABA B receptor agonist baclofen, intrathecal delivery of GABA uptake inhibitor nipecotic acid (Kakinohana, et al., 2006), ii) intrathecal or systemic delivery of AMPA receptor antagonist NGX424 (Hefferan, et al., 2007, Oshiro, et al., 2010), and by systemic or intrathecal treatment with α2 adrenergic agonist tizanidine (Fuchigami, et al., 2011).

In our current study, the effect of intrathecal treatment with baclofen and AMPA receptor antagonist NGX424 was tested in animals with SAE-induced spasticity. As shown, and as in our previous studies which employed a spinal ischemic injury model, a potent anti-spasticity effect after treatment with both baclofen and NGX424 was measured. These data demonstrate that at least in part the SAE-induced spasticity showed similar pharmacology and sensitivity to well-characterized anti-spasticity agents and also pointed to a common mechanism of SAE-induced spasticity, i.e., loss of local segmental inhibition.

Summary

In our current study, we developed and characterized a rat model of spinal arterial air embolism. Similarly as seen in human patients with a neurological type of decompression illness, rats after spinal air embolism displayed a progressive appearance of motor dysfunction frequently combined with quantifiable muscle spasticity. Spinal histopathological changes were characterized by the presence of disseminated necrotic foci localized in both the gray and white matter throughout the lower thoracic to sacral spinal segments. Spinal delivery of baclofen (GABA B receptor agonist) or NGX424 (AMPA receptor antagonist) provided a potent anti-spasticity effect suggesting that loss of segmental inhibition can in part be involved in the development of spasticity after spinal air embolism-induced injury.

Acknowledgments

Support: This work was supported by a grant from the National Institutes of Health (NIH) (NS051644 to MM).

References

Barratt DM, Harch PG, Van Meter K. Decompression illness in divers: a review of the literature. Neurologist. 2002; 8:186–202. [PubMed: 12803690]

Barratt DM, Van Meter K. Decompression sickness in Miskito Indian lobster divers: review of 229 cases. Aviat Space Environ Med. 2004; 75:350–353. [PubMed: 15086125]

Basso DM, Beattie MS, Bresnahan JC, Anderson DK, Faden AI, Gruner JA, Holford TR, Hsu CY, Noble LJ, Nockels R, Perot PL, Salzman SK, Young W. MASCIS evaluation of open field locomotor scores: effects of experience and teamwork on reliability. Multicenter Animal Spinal Cord Injury Study. Journal of Neurotrauma. 1996; 13:343–359. [PubMed: 8863191]

Beard S, Hunn A, Wight J. Treatments for spasticity and pain in multiple sclerosis: a systematic review. Health Technol Assess. 2003; 7:1–124.

Bose P, Parmer R, Thompson FJ. Velocity-dependent ankle torque in rats after contusion injury of the midthoracic spinal cord: time course. J Neurotrauma. 2002; 19:1231–1249. [PubMed: 12427331]

Boulenguez P, Liabeuf S, Bos R, Bras H, Jean-Xavier C, Brocard C, Stil A, Darbon P, Cattaert D, Delpire E, Marsala M, Vinay L. Down-regulation of the potassium-chloride cotransporter KCC2 contributes to spasticity after spinal cord injury. Nat Med. 2010; 16:302–307. [PubMed: 20190766]

Broome JR, Dick EJ Jr. Neurological decompression illness in swine. Aviat Space Environ Med. 1996; 67:207–213. [PubMed: 8775397]

Calder IM, Palmer AC, Hughes JT, Bolt JF, Buchanan JD. Spinal cord degeneration associated with type II decompression sickness: case report. Paraplegia. 1989; 27:51–57. [PubMed: 2922208]

Francis TJ, Griffin JL, Homer LD, Pezeshkpour GH, Dutka AJ, Flynn ET. Bubble-induced dysfunction in acute spinal cord decompression sickness. J Appl Physiol. 1990; 68:1368–1375. [PubMed: 2347778]

Francis TJ, Pezeshkpour GH, Dutka AJ. Arterial gas embolism as a pathophysiologic mechanism for spinal cord decompression sickness. Undersea Biomed Res. 1989; 16:439–451. [PubMed: 2603241]

Fuchigami T, Kakinohana O, Hefferan MP, Lukacova N, Marsala S, Platoshyn O, Sugahara K, Yaksh TL, Marsala M. Potent suppression of stretch reflex activity after systemic or spinal delivery of tizanidine in rats with spinal ischemia-induced chronic spastic paraplegia. Neuroscience. 2011; 194:160–169. [PubMed: 21871540]

Gelfan S. Altered spinal motoneurons in dogs with experimental hind-lamb rigidity. J Neurophysiol. 1966; 29:583–611. [PubMed: 5966426]

Gregersen R, Lambertsen K, Finsen B. Microglia and macrophages are the major source of tumor necrosis factor in permanent middle cerebral artery occlusion in mice. Journal of Cerebral Blood Flow and Metabolism. 2000; 20:53–65. [PubMed: 10616793]

Hallenbeck JM. Cinephotomicrography of dog spinal vessels during cord-damaging decompression sickness. Neurology. 1976; 26:190–199. [PubMed: 943072]

Hefferan MP, Kucharova K, Kinjo K, Kakinohana O, Sekerkova G, Nakamura S, Fuchigami T, Tomori Z, Yaksh TL, Kurtz N, Marsala M. Spinal astrocyte glutamate receptor 1 overexpression after ischemic insult facilitates behavioral signs of spasticity and rigidity. J Neurosci. 2007; 27:11179–11191. [PubMed: 17942713]

Ho SM, Waite PM. Effects of different anesthetics on the paired-pulse depression of the h reflex in adult rat. Exp Neurol. 2002; 177:494–502. [PubMed: 12429194]

Hyldegaard O, Moller M, Madsen J. Protective effect of oxygen and heliox breathing during development of spinal decompression sickness. Undersea Hyperb Med. 1994; 21:115–128. [PubMed: 8061554]

Kakinohana O, Hefferan MP, Nakamura S, Kakinohana M, Galik J, Tomori Z, Marsala J, Yaksh TL, Marsala M. Development of GABA-sensitive spasticity and rigidity in rats after transient spinal cord ischemia: a qualitative and quantitative electrophysiological and histopathological study. Neuroscience. 2006; 141:1569–1583. [PubMed: 16797137]

Kim SW, Kim RC, Choi BH, Gordon SK. Non-traumatic ischaemic myelopathy: a review of 25 cases. Paraplegia. 1988; 26:262–272. [PubMed: 3050797]

Kita M, Goodkin DE. Drugs used to treat spasticity. Drugs. 2000; 59:487–495. [PubMed: 10776831]

Krach LE. Pharmacotherapy of spasticity: oral medications and intrathecal baclofen. J Child Neurol. 2001; 16:31–36. [PubMed: 11225954]

Mabuchi T, Kitagawa K, Ohtsuki T, Kuwabara K, Yagita Y, Yanagihara T, Hori M, Matsumoto M. Contribution of microglia/macrophages to expansion of infarction and response of oligodendrocytes after focal cerebral ischemia in rats. Stroke. 2000; 31:1735–1743. [PubMed: 10884481]

Marsala M, Hefferan MP, Kakinohana O, Nakamura S, Marsala J, Tomori Z. Measurement of peripheral muscle resistance in rats with chronic ischemia-induced paraplegia or morphine-induced rigidity using a semi-automated computer-controlled muscle resistance meter. J Neurotrauma. 2005; 22:1348–1361. [PubMed: 16305323]

Marsala M, Kakinohana O, Yaksh TL, Tomori Z, Marsala S, Cizkova D. Spinal implantation of hNT neurons and neuronal precursors: graft survival and functional effects in rats with ischemic spastic paraplegia. Eur J Neurosci. 2004; 20:2401–2414. [PubMed: 15525281]

Marzella L, Yin A. Role of extravascular gas bubbles in spinal cord injury induced by decompression sickness in the rat. Exp Mol Pathol. 1994; 61:16–23. [PubMed: 7995376]

Matsumoto S, Matsumoto M, Yamashita A, Ohtake K, Ishida K, Morimoto Y, Sakabe T. The temporal profile of the reaction of microglia, astrocytes, and macrophages in the delayed onset paraplegia after transient spinal cord ischemia in rabbits. Anesth Analg. 2003; 96:1777–1784. table of contents. [PubMed: 12761011]

Matsushita A, Smith CM. Spinal cord function in postischemic rigidity in the rat. Brain Research. 1970; 19:395–410. [PubMed: 4315453]

Medby C, Ro H, Koteng S, Juul R, Krossnes BK, Brubakk AO. Microdialysis in cisterna magna during cerebral air embolism in swine. Undersea Hyperb Med. 2002; 29:226–234. [PubMed: 12670124]

Oshiro M, Hefferan MP, Kakinohana O, Lukacova N, Sugahara K, Yaksh TL, Marsala M. Suppression of stretch reflex activity after spinal or systemic treatment with AMPA receptor antagonist NGX424 in rats with developed baclofen tolerance. British Journal of Pharmacology. 2010; 161:976–985. [PubMed: 20977450]

Rubinstein A, Arbit E. Spinal cord blood flow in the rat under normal physiological conditions. Neurosurgery. 1990; 27:882–886. [PubMed: 2274128]

Schievink WI, Luyendijk W, Los JA. Does the artery of Adamkiewicz exist in the albino rat? J Anat. 1988; 161:95–101. [PubMed: 3254897]

Taira Y, Marsala M. Effect of proximal arterial perfusion pressure on function, spinal cord blood flow, and histopathologic changes after increasing intervals of aortic occlusion in the rat. Stroke. 1996; 27:1850–1858. [PubMed: 8841344]

Thompson FJ, Parmer R, Reier PJ. Alteration in rate modulation of reflexes to lumbar motoneurons after midthoracic spinal cord injury in the rat. I Contusion injury. J Neurotrauma. 1998; 15:495–508. [PubMed: 9674553]

Tournebise H, Boucand MH, Landi J, Theobald X. Paraplegia and decompression sickness. Paraplegia. 1995; 33:636–639. [PubMed: 8584297]

Ward CA, McCullough D, Yee D, Stanga D, Fraser WD. Complement activation involvement in decompression sickness of rabbits. Undersea Biomed Res. 1990; 17:51–66. [PubMed: 2316060]

Woolen DHM, MIllen JW. The arterial supply of the spinal cord and its significance. J Neurol Neurosurg Psychiatry. 1955; 18:97–102. [PubMed: 14381918]

Highlights

- Development of a model of spinal cord air embolism-induced injury in rats
- Spinal air embolism leads to progressive development of stretch hyper-reflexia
- Spinal air embolism leads to the loss of rate-dependent depression
- Air embolism-induced stretch hyper-reflexia is blocked by GABA agonist
- Air embolism-induced stretch hyper-reflexia is blocked by AMPA receptor antagonist

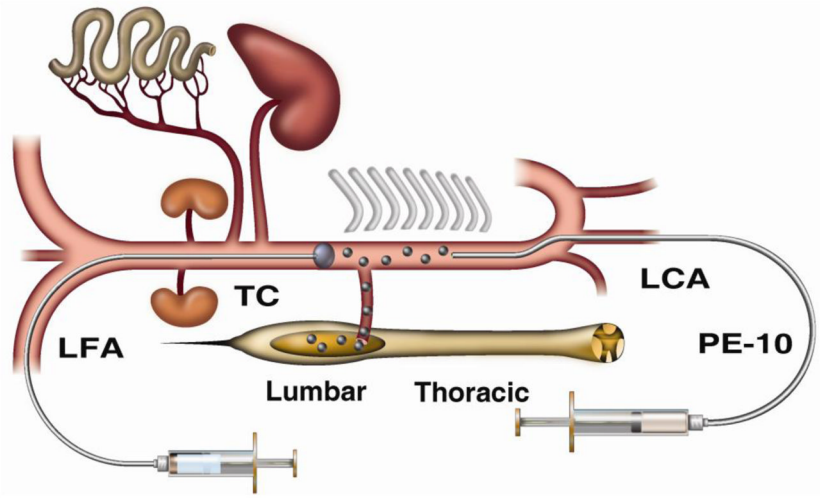

Figure 1. Schematic drawing of the spinal arterial air embolism model in rat

To induce spinal arterial air embolism in isoflurane-anesthetized Sprague-Dawley rats, a PE-10 catheter is placed into the descending thoracic aorta through the left carotid artery (LCA) and air (50, 100, 150 or 200 μl) is injected at a rate of 50 μl/min. To prevent air embolization of other organs and tissues than the spinal cord, a 2F balloon catheter is placed from the left femoral artery (LFA) into the abdominal aorta with the tip of catheter resting above the truncus coeliacus (TC). The balloon is inflated with 0.05 cc of saline just before air injections into the descending thoracic aorta. (Lumbar-lumbar portion of the spinal cord; Thoracic-thoracic portion of the spinal cord).

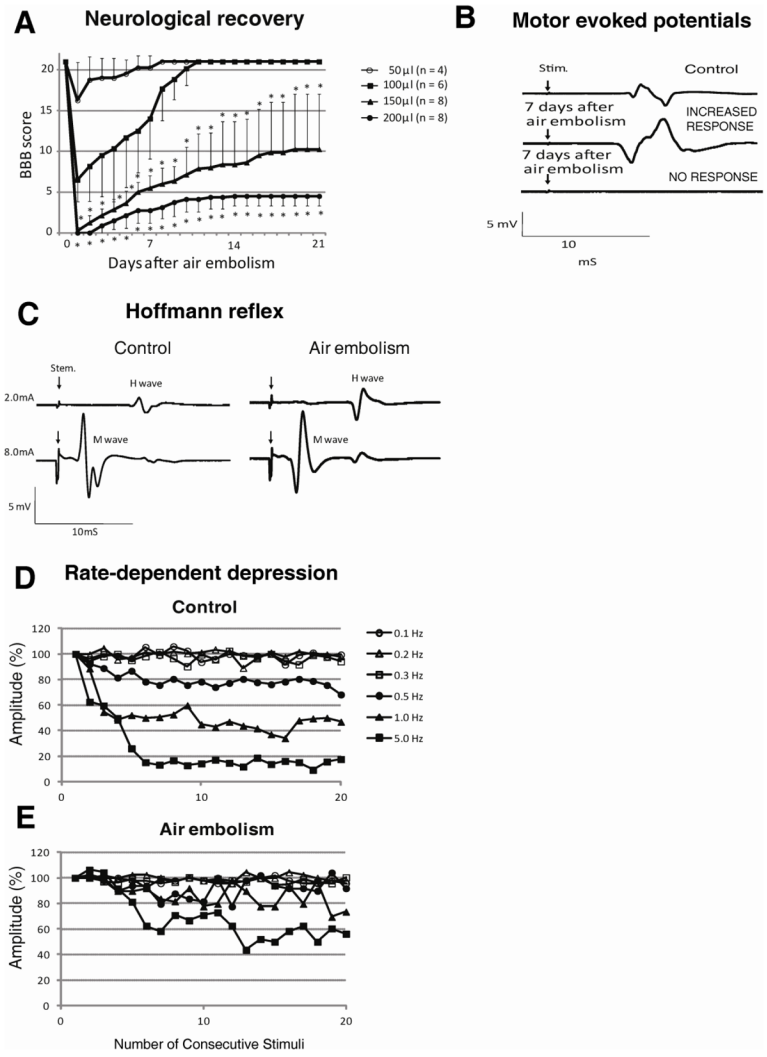

Figure 2. Changes in motor ambulatory function, motor evoked potentials and Hoffmann reflex in rats with spinal air embolism

A: Rats after spinal air embolism showed injected air volume-dependent loss of motor function. Animals injected with 200 μl of air showed near complete loss of motor function (BBB score 3–4.5) and had only partial functional recovery at 3 weeks after air embolism. Animals injected with 50 or 100 μl of air displayed only transient neurological impairment during the first 5–10 days but this was followed by full neurological recovery. Statistical analysis showed a significantly worse neurological score in the 150 and 200 μl groups if compared to the 50 or 100 μl groups (mean±SD; *- $p<0.05$; mixed-design ANOVA).

B: Motor evoked potentials (MEPs) recorded from gastrocnemius muscle in 2 individual animals receiving 200 μl of intra-aortic air injection and surviving for 3 weeks. In the first animal (middle trace), an increase in MEP amplitude was recorded compared to control (see Table 1 for quantitative analysis). In the second animal, using the same stimulation intensity (8 mA), no response was detected.

C, D, E: Hoffman reflex (H-reflex) recorded at 3 weeks after SAE in animals with identified muscle spasticity. Compared to naïve controls, a significant increase in H/M ratio was measured in animals with SAE-induced spasticity (C-compare control to air embolism tracings). Measurement of rate-dependent-depression (RDD) of the H-wave, after

progressively increased rate of peripheral nerve stimulation, showed loss of RDD in animals with SAE-induced spasticity after stimulation frequencies of 0.5, 1.0 and 5.0 Hz (compare control-D to spastic-E) (see Table 2 and 3 for quantitative analysis).

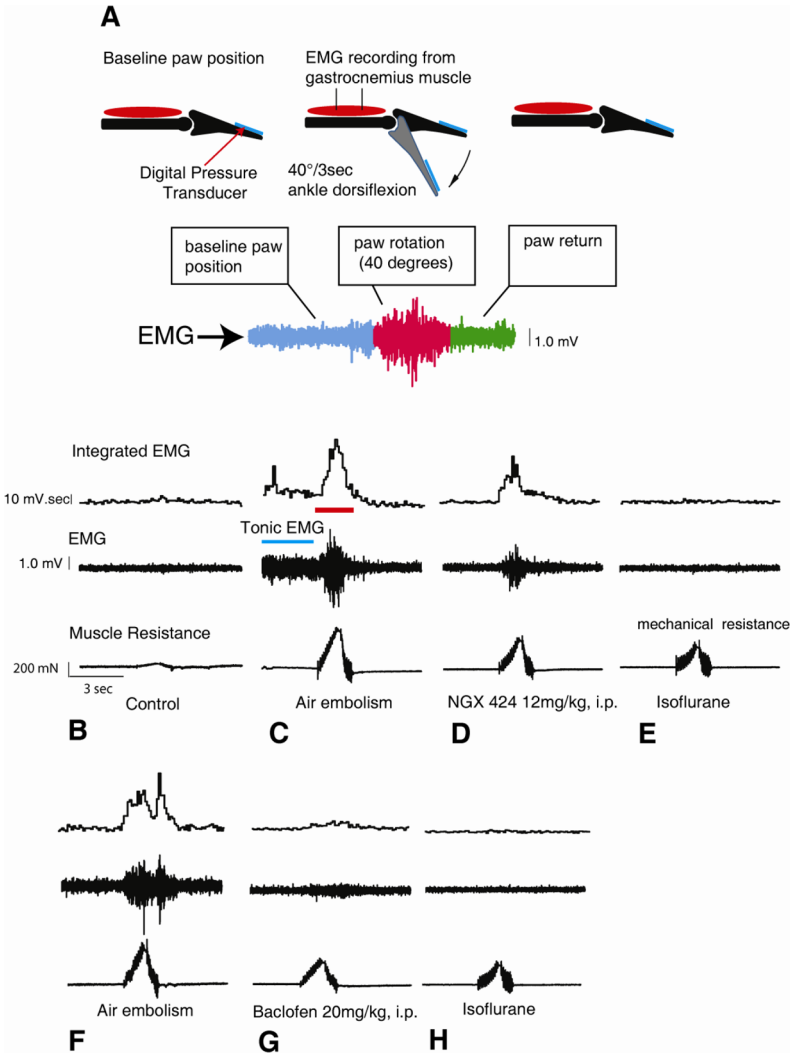

Figure 3. Development of muscle spasticity in animals after spinal air embolism and potent anti-spasticity effect after systemic AMPA receptor antagonist or after GABA B receptor agonist treatment

A–C: To identify the presence of muscle spasticity, fully awake animals are placed into a plastic tube restrainer. Using a computer-controlled ankle rotational system the right ankle is rotated 40°C at velocity of 3 seconds and the muscle resistance measured using a digital pressure transducer (**A**). The EMG signal is recorded from the gastrocnemius muscle using transcutaneously placed needle electrodes during the 3 sec recording trial. Compared to control animals, an increased baseline tonic EMG activity is seen before ankle dorsiflexion (i.e., rigidity) in animals with air-embolism-induced injury (**C**-tonic EMG; blue line) and is then followed by a burst EMG activity and correlative increase in muscle resistance measured during ankle dorsiflexion (i.e., spasticity) (**C**-red line). **D, E:** Systemic treatment with NGX424 (12 mg/kg/i.p.) led to a potent anti-rigidity and anti-spasticity effect at 30 min after drug delivery as defined by suppression of ankle dorsiflexion-induced EMG activity and corresponding suppression in muscle resistance. To identify maximum possible treatment effect, animals are anesthetized with 2% isoflurane at the end of drug-treatment experiment and the residual “mechanical” resistance determined (**E**-mechanical resistance). The value of measured residual resistance is then subtracted from the value measured after drug treatment and the drug related effect calculated and expressed as % of maximum

possible effect (see Fig. 4 for quantitative analysis of anti-spasticity effect). **F–H:** Similarly as seen after NGX424, a potent anti-rigidity and anti-spasticity effect after systemic treatment with baclofen (20 mg/kg/i.p.) was seen (see Fig. 4 for quantitative analysis of anti-spasticity effect).

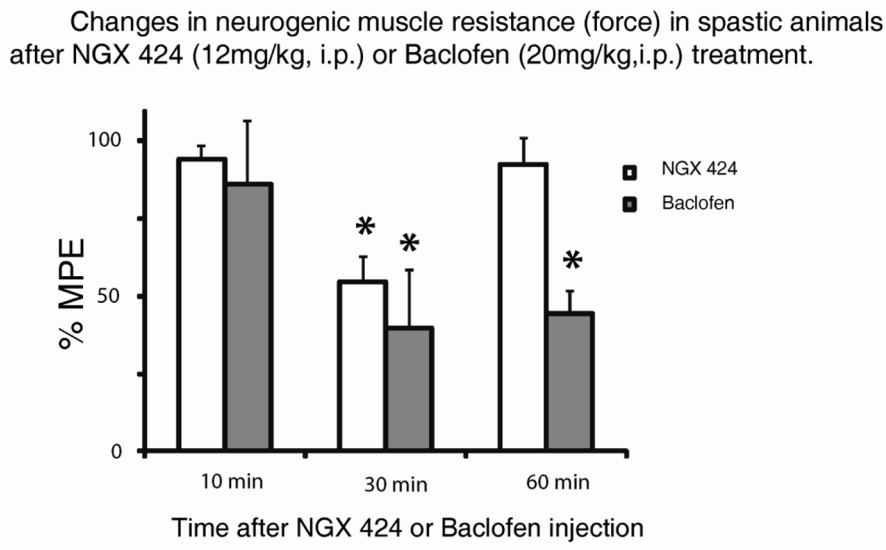

Figure 4. Quantitative analysis of the anti-spasticity effect after systemic AMPA receptor antagonist (NGX 424; 12 mg/kg/i.p.) or GABA B receptor agonist (baclofen; 20 mg/kg/i.p.) treatment

Expressed as a % of maximum possible effect (MPE) measured after isoflurane anesthesia, a significant reduction of muscle resistance (neurogenic component) at 30 min after NGX424 and baclofen delivery was seen (mean±SD; t-test; $p<0.05$).

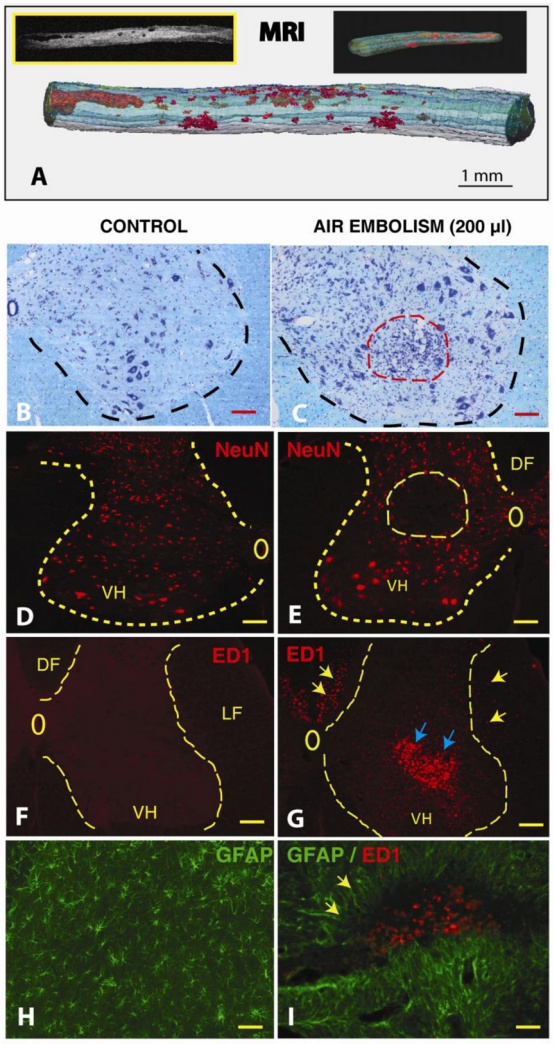

Figure 5. Development of spinal neurodegenerative changes after spinal air embolism

Animals received 200 µl of intra-aortic air injection and survived for 3 weeks. Neurologically, animals developed spastic paraplegia at 4–5 days after air embolism and spasticity persisted for the whole period of 3 weeks survival.

A: After perfusion fixation with 4% paraformaldehyde, the spinal cord was dissected and imaged in situ with 7T-MRI. Low density necrotic foci (BW insert) were readily identified in both the white and gray matter from the mid-thoracic to lumbosacral spinal segments. 3D reconstruction of stack of calibrated MRI images showed the size of necrotic foci between 200 µm to 2–3 mm (red structures). (Scale bar: 1 mm)

B, C: Kl ver-Barrera staining of transverse spinal cord sections taken from upper lumbar region from a control animal (B) or from an animal after air embolism (C). A clear loss of small interneurons and hypercellularity (likely of microglial origin) in the affected region (C: red dashed circle) can be seen. (Scale bars in B, C: 100 µm)

D, E: Immunofluorescence staining with NeuN antibody in a control animal (D) or from an animal after air embolism (E). Compared to control animals, areas of neuronal loss can be identified in animals after spinal air embolism (E: yellow circle). (Scale bars in D, E: 150 µm)

F, G: Immunofluorescence staining with ED1 antibody in a control animal (F) or from an animal with air embolism (G). Compared to control sections which show no ED1+ cellular elements, a clear accumulation of ED+ cells (activated microglia and macrophages) can be identified in the areas of neuronal loss (blue arrows) as well as in the region of the corticospinal tract in the dorsal funiculus (DF) and in lateral funiculus (LF) (yellow arrows). (Scale bars in F, G: 150 μm)

H, I: Double immunofluorescence staining with ED1 and GFAP antibody in a control animal (H) or from an animal after air embolism (I). Compared to control animals, the presence of hypertrophic GFAP+ astrocytes surrounding the ED1 cell-infiltrated regions can be seen. (Scale bars in H, I: 40 μm)

Table 1

Hoffmann reflex in air embolism-induced spastic animals

	Control	Air embolism
M max	8.61 ± 0.26	8.73 ± 0.52
H max	1.95 ± 0.14	3.78 ± 0.38 *
H/M	0.23 ± 0.01	0.43 ± 0.04 *

n = 9, mean ± SE,

* P<0.01

Table 2

Rate-dependent depression in air embolism-induced spastic animals

	impulses	0.1 HZ	0.2 HZ	0.3 Hz	0.5 Hz	1.0 Hz	5.0 Hz
Control	1~10	99.8 ± 1.3	100.0 ± 0.8	97.3 ± 1.1	83.8 ± 2.5**	60.2 ± 5.9**	33.7 ± 9.5**
	11~20	98.3 ± 0.9	98.9 ± 1.3	97.1 ± 1.0	76.7 ± 1.1**	43.5 ± 1.6**	15.1 ± 0.9**
Air embolism	1~10	99.0 ± 0.6	100.2 ± 0.7	98.0 ± 0.8	90.8 ± 2.4*	90.6 ± 2.5*	81.3 ± 5.7**
	11~20	97.5 ± 0.7	100.0 ± 0.9	97.5 ± 0.7	94.1 ± 2.4*	83.7 ± 3.3**	56.9 ± 2.6**

n=9; mean ± SE,

* P<0.05,

** P<0.01 (unpaired t-test)